(Received 30 June 2025, Accepted 11 September 2025, Scheduled 22 September 2025)

Spin Spherical Harmonics for the Analysis of Antenna Electromagnetic Fields

Alice Quennelle[1], Alexandre Chabory[2, *], and Romain Contreres[3]

[1] *Formerly with ENAC lab, Université de Toulouse, Toulouse, France. Now with Thales Six, Gennevilliers, France*
[2] *ENAC lab, Université de Toulouse, Toulouse, France*
[3] *CNES, Toulouse, France*

ABSTRACT: Spherical harmonics are classical analysis tools in many science and engineering domains. For analyzing the electromagnetic fields of antennas in the frequency domain, the mostly used formulation is the one proposed by Hansen. This article proposes an alternative solution, relying on spin spherical harmonics. On a sphere, the tangential components of electric and magnetic fields are represented by means of harmonics of spin ± 1. Then, new closed-form relations are established between spin spherical harmonics and the ones formulated by Hansen. A sampling theorem and fast transforms that are consistent with spin spherical harmonics are used. The radiations of spin spherical harmonics of order 1 are related to elementary dipoles and Huygens sources in circular polarization. Finally, numerical experiments are performed with a horn antenna and a GNSS antenna installed on an aircraft. They show that a very large radiating system with a band-limit of 2048 can be efficiently analyzed by means of fast spin spherical harmonic transforms, with a computation time of 2 minutes, approximately.

1. INTRODUCTION

Spherical harmonics are commonly used in electromagnetics to analyze and process radiated or scattered fields expressed on a sphere. Formulations of vector spherical harmonics suitable with Maxwell time-harmonic equations are detailed in classical books [1–3]. In the context of antenna measurements, spherical harmonics are widely used to perform near-field to far-field transforms, possibly accounting for the presence of the probe. In this domain, the mostly-used formulation is the one proposed by Hansen [4].

Spherical harmonics are prominent in many other science and engineering fields. Indeed, data are often represented on spheres in computer graphics [5], chemistry [6, 7], geophysics [8–10], planetary science [11, 12], solar physics and astrophysics [13, 14], among many others. For spherical vector data, vector spherical harmonics can be introduced from scalar harmonics by means of potentials via Helmholtz decomposition [1–4]. Alternatively and more generally, the representation of non-scalar spherical data, e.g. vector fields or tensors, typically depends on the orientation of a local frame. This justifies the use of spin spherical harmonics that inherently capture how the data transforms under local rotations. These harmonics have been introduced by Newman and Penrose in [15] to describe gravitational radiation. They are convenient for representing several types of signals on the sphere. The spin of order 0 is suitable for describing scalar signals, while the spins of order ± 1 allow the representation of vector fields tangential to the sphere. In mathematical physics, spherical harmonics of spins 0 and ± 1 have been considered in [16, 17] for analyzing the solution of Maxwell equations in spherical coordinates. Higher-order spins can be notably used to characterize higher-order tensors. For example, the anisotropy of cosmic microwave background has been recently studied on a sphere and analyzed in terms of ± 2 spin spherical harmonics [14].

To perform discrete spherical transforms, a sampling of the problem is required. By definition, band-limited signals are signals that can be represented by harmonics of order $n < N$, where N is the band limit. This finiteness in the number of harmonics can be interpreted as a limit in the speed of the variations of the signal. Similar to the sampling theory established by Shannon [18], several sampling grids have been constructed for the exact representation of a band-limited signal in terms of scalar spherical harmonics. This has led to the regular θ-ϕ grid associated with Gauss-Legendre quadrature that requires $\sim 2N^2$ sampling points [19]. The sampling theorem on the sphere of Driscoll & Healy [20] is also commonly used, which requires roughly $\sim 4N^2$ samples on the sphere. Another sampling theorem, proposed by McEwen and Wiaux [21], involves a regular grid with a number of samples of $\sim 2N^2$. Besides, this theorem is consistent with spin spherical harmonics, and fast transforms exist that are both stable and fast, even for harmonics of very large orders. Other samplings that are not based on a regular θ-ϕ grid exist. They offer great flexibility [22, 23]. In electromagnetics, approaches have been proposed to apply them on incomplete (phaseless) data [24]. Nevertheless, they do not provide an exact representation and do not come with fast transforms.

The objective of this article is to analyze the use of spin spherical harmonics to describe antenna radiation. Closed-formed expressions, which are formulated in a matrix form, are

* Corresponding author: Alexandre Chabory (alexandre.chabory@enac.fr).

proposed to relate the representation of a signal by means of spin and Hansen spherical harmonics. Illustrations and tests are presented for different types of antennas, which radiated fields come either from theory or simulation.

The plan of this article is as follows. In Section 2, the theory of spin spherical harmonics is presented. The sampling theorem and fast algorithms that allow the computation of the spin spherical harmonic transform are also described. In Section 3, spin harmonics are applied to electromagnetic radiation, and the relation between the Hansen and the spin spherical representation is derived. Then, in Section 4, spin harmonics of order $n = 1$ are related to elementary dipoles and Huygens sources in circular polarization. Finally, in Section 5, numerical experiments are presented and discussed.

2. THEORY OF SPIN SPHERICAL HARMONICS

2.1. Spin Functions

Spin functions are particular elements of the space of square integrable functions on the sphere, denoted as $L^2(S^2)$, where S^2 is the unit sphere, i.e., the sphere of radius 1. They are parameterized by a spin order $s \in \mathbb{Z}$. A spin function u_s is characterized by its behavior under a local rotation [21], i.e., a rotation by $\chi_\ell \in [0, 2\pi[$ in the tangent plane centered on any spherical coordinates (θ, ϕ), with $\theta \in [0, \pi]$ and $\phi \in [0, 2\pi[$. Indeed, local rotations yield a spin dependent phase shift given by

$$u'_s(\theta, \phi) = e^{-is\chi_\ell} u_s(\theta, \phi), \tag{1}$$

where the prime designates the local rotation of u_s by $\chi_\ell \in [0, 2\pi[$. This is a local rotation as every point on the sphere is associated with a different rotation, whereas a global rotation consists in shifting the entire signal on the sphere and could be represented by an element of the group of rotations SO(3).

2.2. Spin Spherical Harmonics

Several conventions exist for scalar spherical harmonics, which differ from the normalization and the presence of Condon-Shortley phase. Differences notably exist between the convention used for spin spherical harmonics [21] and the one used in the antenna domain by Hansen [4]. In this article, scalar spherical harmonics are written as

$$Y_{m,n}(\theta, \phi) = \frac{1}{\sqrt{2\pi}} \bar{P}_n^m(\cos\theta) e^{im\phi}, \tag{2}$$

where indices n and m are integers so that $n \geq 0$ and $|m| \leq n$. Furthermore, the normalized associated Legendre functions $\bar{P}_n^m$ are defined by

$$\bar{P}_n^m(x) = \sqrt{\frac{2n+1}{2} \frac{(n-m)!}{(n+m)!}} P_n^m(x). \tag{3}$$

Consistent with [21], the Condon-Shortley phase convention, which amounts to a multiplication by $(-1)^m$, is here included in the definition of the associated Legendre functions, i.e.,

$$P_n^m(x) = \frac{(-1)^m}{2^n n!} (1 - x^2)^{m/2} \frac{d^{n+m}}{dx^{n+m}} (x^2 - 1)^n. \tag{4}$$

Spin spherical harmonics are noted as $Y_{s,m,n} \in L^2(S^2)$ with $s \in \mathbb{Z}$, $n \geq |s|$, and $|m| \leq n$. They can be expressed from scalar spherical harmonics using the spin raising and lowering operators, $\eth$ (pronounced "eth") and $\bar{\eth}$, defined by

$$\begin{aligned} \eth &\equiv -\sin^s\theta \left(\frac{\partial}{\partial\theta} + \frac{i}{\sin\theta} \frac{\partial}{\partial\phi} \right) \sin^{-s}\theta, \\ \bar{\eth} &\equiv -\sin^{-s}\theta \left(\frac{\partial}{\partial\theta} - \frac{i}{\sin\theta} \frac{\partial}{\partial\phi} \right) \sin^{s}\theta, \end{aligned} \tag{5}$$

with s the spin order of the signal to which $\eth$ or $\bar{\eth}$ is applied. Spin spherical harmonics are related to scalar (spin-zero) harmonics by

$$\begin{aligned} Y_{s,m,n} &= \sqrt{\tfrac{(n-s)!}{(n+s)!}}\, \eth^s Y_{m,n}, && \text{for } s \geq 0, \\ Y_{s,m,n} &= (-1)^s \sqrt{\tfrac{(n+s)!}{(n-s)!}}\, \bar{\eth}^{-s} Y_{m,n}, && \text{for } s \leq 0, \end{aligned} \tag{6}$$

where $\eth^s$ and $\bar{\eth}^{-s}$ mean that the operators are applied $|s|$ times. In this article, functions of spin $s = \{-1, 0, 1\}$ are considered.

From (6) and (2), the ± 1 spin harmonics are expressed as

$$\begin{aligned} Y_{-1,m,n} &= \frac{e^{im\phi}}{\sqrt{2\pi}\sqrt{n(n+1)}} \left(\frac{\mathrm{d}}{\mathrm{d}\theta} + \frac{m}{\sin\theta} \right) \bar{P}_n^m(\cos\theta), \\ Y_{+1,m,n} &= \frac{-e^{im\phi}}{\sqrt{2\pi}\sqrt{n(n+1)}} \left(\frac{\mathrm{d}}{\mathrm{d}\theta} - \frac{m}{\sin\theta} \right) \bar{P}_n^m(\cos\theta). \end{aligned} \tag{7}$$

Spin spherical harmonics form an orthogonal basis for $L^2(S^2)$ spin-s functions. Thus, any square integrable spin s function $u_s(\theta, \phi)$ can be written as

$$u_s(\theta, \phi) = \sum_{n=|s|}^{\infty} \sum_{m=-n}^{n} C_{m,n}^s Y_{s,m,n}(\theta, \phi), \tag{8}$$

with $C_{m,n}^s$ the spin spherical harmonic coefficients given by

$$C_{m,n}^s = \langle u_s, Y_{s,m,n} \rangle, \tag{9}$$

and where $\langle , \rangle$ is the $L^2(S^2)$ inner product. Thus, we have

$$\begin{aligned} C_{m,n}^s &= \iint_{S^2} u_s(\theta, \phi) v_{s,m,n}^*(\theta, \phi) dS \\ &= \int_0^{\pi} \int_0^{2\pi} u_s(\theta, \phi) Y_{s,m,n}^*(\theta, \phi) \sin\theta d\theta d\phi. \end{aligned} \tag{10}$$

2.3. Spin Components of a Vector Field

Any vector field $\boldsymbol{V}$ defined on the unit sphere S^2 can be expanded on radial and tangential components as

$$\boldsymbol{V} = \boldsymbol{V}_t + \boldsymbol{V}_r. \tag{11}$$

The tangential component $\boldsymbol{V}_t$ can be formulated as

$$\boldsymbol{V}_t(\theta, \phi) = V_{-1}(\theta, \phi) \hat{\boldsymbol{u}}_{-1} + V_{+1}(\theta, \phi) \hat{\boldsymbol{u}}_{+1}, \tag{12}$$

with

$$\hat{\boldsymbol{u}}_{-1} = \frac{\hat{\boldsymbol{\theta}} + i\hat{\boldsymbol{\phi}}}{\sqrt{2}}, \qquad \hat{\boldsymbol{u}}_{+1} = \frac{\hat{\boldsymbol{\theta}} - i\hat{\boldsymbol{\phi}}}{\sqrt{2}}, \tag{13}$$

where $\hat{\boldsymbol{\theta}}$, $\hat{\boldsymbol{\phi}}$ are the local spherical unit vectors. The unit vectors $\hat{\boldsymbol{u}}_{-1}$ and $\hat{\boldsymbol{u}}_{+1}$ are invariant up to a phase term under a local rotation. This can be demonstrated by noticing that a local rotation of angle χ_l modifies $\hat{\boldsymbol{\theta}}$ and $\hat{\boldsymbol{\phi}}$ as follows

$$\hat{\boldsymbol{\theta}}' = \cos\chi_\ell \hat{\boldsymbol{\theta}} + \sin\chi_\ell \hat{\boldsymbol{\phi}}, \qquad \hat{\boldsymbol{\phi}}' = -\sin\chi_\ell \hat{\boldsymbol{\theta}} + \cos\chi_\ell \hat{\boldsymbol{\phi}}. \tag{14}$$

From (13), we then have

$$\hat{\boldsymbol{u}}'_{-1} = e^{-i\chi_\ell}\hat{\boldsymbol{u}}_{-1}, \qquad \hat{\boldsymbol{u}}'_{+1} = e^{i\chi_\ell}\hat{\boldsymbol{u}}_{+1}. \tag{15}$$

Consequently, under a local rotation, the components in (12) become

$$V'_{-1} = \boldsymbol{V}_{\mathrm{t}} \cdot \hat{\boldsymbol{u}}'^{*}_{-1} = V_{-1}e^{i\chi_\ell}, \qquad V'_{+1} = \boldsymbol{V}_{\mathrm{t}} \cdot \hat{\boldsymbol{u}}'^{*}_{+1} = V_{+1}e^{-i\chi_\ell}. \tag{16}$$

This means that $V_{-1}(\theta,\phi)$ and $V_{+1}(\theta,\phi)$ are of spin -1 and spin $+1$, respectively. Thus, from (12), the tangential field components can be written as a sum of ± 1 spin spherical harmonics, which explicitly corresponds to

$$\boldsymbol{V}_{\mathrm{t}}(\theta,\phi) = \sum_{n=1}^{\infty}\sum_{m=-n}^{n} V_{-1,m,n}Y_{-1,m,n}\hat{\boldsymbol{u}}_{-1} + V_{+1,m,n}Y_{+1,m,n}\hat{\boldsymbol{u}}_{+1}. \tag{17}$$

As for the radial component of $\boldsymbol{V}$, it is unchanged under local rotation. Thus, the radial component of a vector field can be described by means of spherical harmonics of spin 0. Nevertheless, in this article, the radial component is not considered, as the entire field can be characterized from the tangential components, according to the unicity theorem [1].

The unit vectors in (13) show a strong resemblance to the unit vectors associated with left-hand and right-hand circular polarizations. This means that in the far-field zone, a representation on $s = \pm 1$ unit vectors is only about expanding the field on the right-hand and left-hand circular components.

Spin signals also present a global rotation property, or rotation over the sphere, which induces a particular phase shift [25].

2.4. Fast Spin Spherical Harmonics Transform

Any physical signal on a sphere, in particular the electromagnetic fields radiated by an antenna, has limited variations and can thus be exactly represented by means of a finite number of harmonics. Such signals are said to be band-limited. The summations over n are then truncated to $N-1$, where N is called the band limit. McEwen and Wiaux [21] have proposed a sampling theorem and fast spin spherical harmonic transforms for band-limited spin signals. They allow to represent exactly band-limited signals by means of fast Fourier transforms. In this section, the key-elements of these transforms are presented.

For a signal of band-limit N, using the relation between spin spherical harmonics and Wigner d-functions, the spin spherical transform can be written as

$$C^s_{m,n} = \frac{i^{m+s}}{(-1)^s}\sqrt{\frac{2n+1}{4\pi}}\sum_{q=-(N-1)}^{N-1}\Delta^n_{q,m}\Delta^n_{q,-s}G^s_{m,q}, \tag{18}$$

where $\Delta^n_{m'm}$ are the Wigner d-functions evaluated in $\pi/2$, and

$$G^s_{m,q} = \int_0^{\pi}\int_0^{2\pi} u_s(\theta,\phi)e^{-im\phi-iq\theta}\sin\theta d\theta d\phi. \tag{19}$$

Similarly, the inverse transform can be expressed as

$$u_s(\theta,\phi) = \sum_{q=-(N-1)}^{N-1}\sum_{m=-(N-1)}^{N-1} U^s_{m,q}e^{im\phi+iq\theta}, \tag{20}$$

where

$$U^s_{m,q} = \frac{i^{-(m+s)}}{(-1)^s}\sum_{n=0}^{N-1}\sqrt{\frac{2n+1}{4\pi}}\Delta^n_{q,m}\Delta^n_{q,-s}C^s_{m,q}. \tag{21}$$

To perform discrete transforms, a sampling of the sphere is required. For a signal of band-limit N, the sampling theorem of McEwen & Wiaux is based on an equiangular θ-ϕ grid given by

$$\theta^N_{p_\theta} = \frac{\pi(2p_\theta+1)}{2N-1}, \quad \text{for } p_\theta \in \{0,1,\ldots,N-1\}, \qquad \phi^N_{p_\phi} = \frac{2\pi p_\phi}{2N-1}, \quad \text{for } p_\phi \in \{0,1,\ldots,2N-2\}, \tag{22}$$

After this sampling of the sphere, the computations of (19) and (20) amount to discrete Fourier series provided that a periodic extension in θ from $[0,\pi]$ to $[0,2\pi]$ is provided [21]. This extension is defined from the symmetries that the signal has to respect. Finally, the forward transform consists in computing:

- two 2-dimensional fast Fourier transforms along p_θ and p_ϕ of complexity $\mathcal{O}(N^2\log_2 N)$;
- the sum in (18) of complexity $\mathcal{O}(N^3)$.

The overall complexity of the forward transform is dominated by the second part and is thus in $\mathcal{O}(N^3)$. To perform the inverse transform, i.e., to obtain $u_s(\theta_p, \phi_q)$ from the coefficients $C^s_{m,n}$ using (20) and (21), similar steps are followed with a similar complexity. McEwen and Wiaux have demonstrated that using the method of Risbo to compute by recursion of the Wigner d-functions, and the transforms remain stable with an accuracy that goes approximately to the machine precision for band-limit up to $N = 2^{12} = 4096$. Other recursion schemes have been recently investigated to propose fast spin spherical transforms in the framework of differentiable programming [23].

3. APPLICATION TO ELECTROMAGNETIC RADIATION

In this section, spin spherical harmonics are applied to the tangential components of an electromagnetic field on a sphere of radius r in a linear, homogeneous, isotropic medium. Then, closed-form expressions are obtained to formulate the correspondence with Hansen spherical harmonics. The calculations are performed in the frequency domain, the time dependency in $e^{i\omega t}$, with ω, the angular frequency, being omitted.

3.1. Spin Spherical Harmonics

In this section, the spherical harmonic transforms are applied to the following tangential vectors

$$\frac{r}{\sqrt{\zeta}}\boldsymbol{E}_{\mathrm{t}}(r,\theta,\phi) \quad \text{and} \quad -ir\sqrt{\zeta}\boldsymbol{H}_{\mathrm{t}}(r,\theta,\phi), \tag{23}$$

where ζ is the medium wave impedance. The constants are chosen so that spin coefficients associated with $\boldsymbol{E}_{\mathrm{t}}$ and $\boldsymbol{H}_{\mathrm{t}}$ are of unit $[\mathrm{Watt}]^{1/2}$ and are of the same order of magnitude. As explained in Section 2.3, any field transverse to the sphere can be expanded into two components of spin ±1, which, in turns, can be represented as a sum of spherical harmonics of spin ±1. Doing so, the tangential fields in (23) are expressed as

$$\begin{aligned}\boldsymbol{E}_{\mathrm{t}}(r,\theta,\phi) &= \frac{\sqrt{\zeta}}{r}\sum_{s,m,n} C^{\mathrm{E},s}_{m,n}(r)\, Y_{s,m,n}(\theta,\phi)\, \hat{\boldsymbol{u}}_s(\theta,\phi),\\ \boldsymbol{H}_{\mathrm{t}}(r,\theta,\phi) &= \frac{i}{r\sqrt{\zeta}}\sum_{s,m,n} C^{\mathrm{H},s}_{m,n}(r)\, Y_{s,m,n}(\theta,\phi)\, \hat{\boldsymbol{u}}_s(\theta,\phi),\end{aligned} \tag{24}$$

with $C^{\mathrm{E},s}_{m,n}$ and $C^{\mathrm{H},s}_{m,n}$ the spin coefficients associated with the transverse fields $\boldsymbol{E}_{\mathrm{t}}$ and $\boldsymbol{H}_{\mathrm{t}}$, respectively. They are given by

$$\begin{aligned}C^{\mathrm{E},s}_{m,n}(r) &= \frac{r}{\sqrt{\zeta}}\left\langle \boldsymbol{E}_{\mathrm{t}},\ Y_{s,m,n}\hat{\boldsymbol{u}}_s\right\rangle\\ &= \frac{r}{\sqrt{\zeta}}\iint_{S^2}\boldsymbol{E}_{\mathrm{t}}\cdot\left(Y_{s,m,n}\hat{\boldsymbol{u}}^*_s\right)dS,\\ C^{\mathrm{H},s}_{m,n}(r) &= -ir\sqrt{\zeta}\left\langle \boldsymbol{H}_{\mathrm{t}},\ Y_{s,m,n}\hat{\boldsymbol{u}}_s\right\rangle\\ &= -ir\sqrt{\zeta}\iint_{S^2}\boldsymbol{H}_{\mathrm{t}}\cdot\left(Y_{s,m,n}\hat{\boldsymbol{u}}_s\right)^* dS.\end{aligned} \tag{25}$$

3.2. Relation with Hansen Harmonic Coefficients

In antenna domain, the mostly used formulation of spherical harmonics is the one proposed by Hansen. In this article, this formulation is used with slight modifications that are deemed necessary to include the Condon-Shortley phase in the Legendre associated functions as it is classically done for spin spherical harmonics, to be consistent with a time dependency in $e^{i\omega t}$ and to remain as concise as possible. The transverse electric and magnetic fields are written as

$$\begin{aligned}\boldsymbol{E}_{\mathrm{t}} &= \sum_{p=\mathrm{TE,TM}}\sum_{c=1}^{2}\sum_{n=1}^{\infty}\sum_{m=-n}^{n} Q^{p,c}_{m,n}\boldsymbol{e}^{p,c}_{\mathrm{t}\,m,n}(r,\theta,\phi),\\ \boldsymbol{H}_{\mathrm{t}} &= \sum_{p=\mathrm{TE,TM}}\sum_{c=1}^{2}\sum_{n=1}^{\infty}\sum_{m=-n}^{n} Q^{p,c}_{m,n}\boldsymbol{h}^{p,c}_{\mathrm{t}\,m,n}(r,\theta,\phi),\end{aligned} \tag{26}$$

where $Q^{p,c}_{m,n}$ are the harmonic coefficients, and $c = 1$ or 2 correspond to ingoing and outgoing fields, respectively. Besides, $\boldsymbol{e}^{p,c}_{\mathrm{t}\,m,n}$ and $\boldsymbol{h}^{p,c}_{\mathrm{t}\,m,n}$ are the spherical harmonics transverse electric and magnetic fields, respectively. They correspond to

$$\begin{aligned}\boldsymbol{e}^{\mathrm{TE},c}_{\mathrm{t}\,m,n} &= k\sqrt{\zeta}A_n h^{(c)}_n(kr)e^{im\phi}\left[\frac{im}{\sin\theta}\hat{\boldsymbol{\theta}} - \frac{\mathrm{d}\cdot}{\mathrm{d}\theta}\hat{\boldsymbol{\phi}}\right]\bar{P}^m_n(\cos\theta),\\ \boldsymbol{e}^{\mathrm{TM},c}_{\mathrm{t}\,mn} &= k\sqrt{\zeta}A_n w^{(c)}_n(kr)\ e^{im\phi}\left[\frac{\mathrm{d}\cdot}{\mathrm{d}\theta}\hat{\boldsymbol{\theta}} + \frac{im}{\sin\theta}\hat{\boldsymbol{\phi}}\right]\bar{P}^m_n(\cos\theta),\end{aligned} \tag{27}$$

and

$$\begin{aligned}\boldsymbol{h}^{\mathrm{TE},c}_{\mathrm{t}\,m,n} &= \frac{ikA_n}{\sqrt{\zeta}}w^{(c)}_n(kr)e^{im\phi}\left[\frac{\mathrm{d}\cdot}{\mathrm{d}\theta}\hat{\boldsymbol{\theta}} + \frac{im}{\sin\theta}\hat{\boldsymbol{\phi}}\right]\bar{P}^m_n(\cos\theta),\\ \boldsymbol{h}^{\mathrm{TM},c}_{\mathrm{t}\,m,n} &= \frac{ikA_n}{\sqrt{\zeta}}h^{(c)}_n(kr)e^{im\phi}\left[\frac{im}{\sin\theta}\hat{\boldsymbol{\theta}} - \frac{\mathrm{d}\cdot}{\mathrm{d}\theta}\hat{\boldsymbol{\phi}}\right]\bar{P}^m_n(\cos\theta),\end{aligned} \tag{28}$$

where

$$A_n = \frac{1}{\sqrt{2\pi n(n+1)}}. \tag{29}$$

Furthermore, $h^{(c)}_n$ are the spherical Hankel functions, and $w^{(c)}_n$ are related to their derivatives according to

$$w^{(c)}_n(kr) = \frac{1}{kr}\frac{\mathrm{d}}{\mathrm{d}(kr)}\left(kr\ h^{(c)}_n(kr)\right). \tag{30}$$

The relations between the spin and Hansen spherical harmonic coefficients are now derived. For the sake of simplicity, only the calculation of $+1$ spin coefficients of the electric field are detailed. Inserting the Hansen expansion (26) in (25) and using linearity, these coefficients are written as

$$C^{\mathrm{E},1}_{m',n'}(r) = \frac{r}{\sqrt{\zeta}}\sum_{p,c,m,n} Q^{p,c}_{m,n}\left\langle \boldsymbol{e}^{p,c}_{\mathrm{t}\,m,n}\ ,\ \ Y_{1,m',n'}\hat{\boldsymbol{u}}_1\right\rangle, \tag{31}$$

with

$$\left\langle \boldsymbol{e}_{\mathrm{t}\,m,n}^{p,c}, Y_{1,m',n'}\hat{\boldsymbol{u}}_1 \right\rangle = \iint_{S^2} \boldsymbol{e}_{\mathrm{t}\,m,n}^{p,c} \cdot \left(Y_{1,m',n'}\hat{\boldsymbol{u}}_1\right)^* dS. \tag{32}$$

From (27), (13), and (7), we have

$$\begin{aligned} \boldsymbol{e}_{\mathrm{t}\,m,n}^{\mathrm{TE},c} \cdot \hat{\boldsymbol{u}}_1^* &= ik\sqrt{\frac{\zeta}{2}} s_m h_n^{(c)}(kr) Y_{1,m,n} \\ \boldsymbol{e}_{\mathrm{t}\,m,n}^{\mathrm{TM},c} \cdot \hat{\boldsymbol{u}}_1^* &= -k\sqrt{\frac{\zeta}{2}} s_m w_n^{(c)}(kr) Y_{1,m,n}. \end{aligned} \tag{33}$$

Then, using the orthogonality of the spin spherical harmonics, we end up with

$$\begin{aligned} \left\langle \boldsymbol{e}_{\mathrm{t}\,m,n}^{\mathrm{TE},c}, Y_{1,m',n'}\hat{\boldsymbol{u}}_1 \right\rangle &= ik\sqrt{\frac{\zeta}{2}} h_n^{(c)}(kr)\delta_{m,m'}\delta_{n,n'}, \\ \left\langle \boldsymbol{e}_{\mathrm{t}\,m,n}^{\mathrm{TM},c}, Y_{1,m',n'}\hat{\boldsymbol{u}}_1 \right\rangle &= -k\sqrt{\frac{\zeta}{2}} w_n^{(c)}(kr)\delta_{m,m'}\delta_{n,n'}, \end{aligned} \tag{34}$$

where δ stands for the Kronecker symbol. From this result, (31) reduces to

$$\begin{aligned} C_{m,n}^{\mathrm{E},1}(r) = \frac{kr}{\sqrt{2}} \Big[& ih_n^{(1)}(kr) Q_{m,n}^{\mathrm{TE},1} + ih_n^{(2)}(kr) Q_{m,n}^{\mathrm{TE},2} \\ & - Q_{m,n}^{\mathrm{TM},1} w_n^{(1)}(kr) - Q_{m,n}^{\mathrm{TM},(2)} w_n^{(2)}(kr) \Big]. \end{aligned} \tag{35}$$

This equation provides the $+1$ spin coefficients of the electric field from the Hansen coefficients. Similar derivations can be performed in order to obtain the other spin coefficients. The final relations can be gathered in a matrix form given by

$$\begin{bmatrix} C_{m,n}^{\mathrm{E},-1} \\ C_{m,n}^{\mathrm{E},+1} \\ C_{m,n}^{\mathrm{H},-1} \\ C_{m,n}^{\mathrm{H},+1} \end{bmatrix} = \frac{kr}{\sqrt{2}} \begin{bmatrix} ih_n^{(1)} & w_n^{(1)} & ih_n^{(2)} & w_n^{(2)} \\ ih_n^{(1)} & -w_n^{(1)} & ih_n^{(2)} & -w_n^{(2)} \\ w_n^{(1)} & ih_n^{(1)} & w_n^{(2)} & ih_n^{(2)} \\ -w_n^{(1)} & ih_n^{(1)} & -w_n^{(2)} & ih_n^{(2)} \end{bmatrix} \begin{bmatrix} Q_{m,n}^{\mathrm{TE},1} \\ Q_{m,n}^{\mathrm{TM},1} \\ Q_{m,n}^{\mathrm{TE},2} \\ Q_{m,n}^{\mathrm{TM},2} \end{bmatrix}. \tag{36}$$

The inverse matrix is calculated by means of a Gaussian elimination and properties of the Wronskian associated with spherical Hankel functions

$$w_n^{(2)}(kr)h_n^{(1)}(kr) - w_n^{(1)}(kr)h_n^{(2)}(kr) = \frac{-2i}{(kr)^2}. \tag{37}$$

Hence, the matrix to obtain the Hansen coefficients from the spin coefficients is

$$\begin{bmatrix} Q_{m,n}^{\mathrm{TE},1} \\ Q_{m,n}^{\mathrm{TM},1} \\ Q_{m,n}^{\mathrm{TE},2} \\ Q_{m,n}^{\mathrm{TM},2} \end{bmatrix} = \frac{kr}{2\sqrt{2}} \begin{bmatrix} w_n^{(2)} & w_n^{(2)} & -ih_n^{(2)} & ih_n^{(2)} \\ -ih_n^{(2)} & ih_n^{(2)} & w_n^{(2)} & w_n^{(2)} \\ -w_n^{(1)} & -w_n^{(1)} & ih_n^{(1)} & -ih_n^{(1)} \\ ih_n^{(1)} & -ih_n^{(1)} & -w_n^{(1)} & -w_n^{(1)} \end{bmatrix} \begin{bmatrix} C_{m,n}^{\mathrm{E},+1} \\ C_{m,n}^{\mathrm{E},-1} \\ C_{m,n}^{\mathrm{H},+1} \\ C_{m,n}^{\mathrm{H},-1} \end{bmatrix}. \tag{38}$$

Finally, we have obtained a rigorous formulation, in the form of an invertible matrix, to go from spin to Hansen representations, and the other way around. In the far-field zone, this matrix can be simplified by replacing the Hansen functions h_n and w_n by their asymptotic approximation valid for $kr \gg n$

$$\begin{aligned} h_n^{(1)}(kr) &\sim (-i)^{n+1}\frac{e^{ikr}}{kr}, \quad & w_n^{(1)}(kr) &\sim (-i)^{n}\frac{e^{ikr}}{kr}, \\ h_n^{(2)}(kr) &\sim i^{n+1}\frac{e^{-ikr}}{kr}, \quad & w_n^{(2)}(kr) &\sim i^{n}\frac{e^{-ikr}}{kr}. \end{aligned} \tag{39}$$

3.3. Comparative Analysis

To conclude this section, a comparative analysis is performed between Hansen and spin spherical harmonics in Table 1. Hansen harmonics rely on the potential theory which yields harmonics that are either TE or TM. They incorporate the propagation along r. They are normalized in terms of the active power (each harmonic carries 1/2 W). On the other hand, spin harmonics rely on local rotations. For ± 1 spin, this yields vector fields whose structure amounts to both circular polarizations. They are normalized in $L^2(S^2)$ and do not include the propagation in r, but a sampling theorem and associated exact fast transforms exist for band-limited signals.

TABLE 1. Comparative analysis between Hansen and spin spherical harmonics.

	Theory	Polar.	Propag.	Norm	Sampling th.
Hansen	potential	TE/TM	✓	active power	×
Spin	local rot.	circular	×	$L^2(S^2)$	✓

4. RADIATION ASSOCIATED WITH SPIN SPHERICAL HARMONICS OF ORDER n = 1

In this section, the radiation of spin spherical harmonics of order $n = 1$ is related to elementary dipoles and Huygens sources in circular polarization. For the sake of conciseness, only coefficients associated with the electric field are presented.

4.1. Spin Spherical Harmonics So That n = 1 and m = 0

For Hansen spherical harmonics, it is well known that an elementary electric dipole oriented along z and located at the origin only radiates one TM harmonic so that $n = 1$ and $m = 0$ [4]. The coefficient is given by

$$Q_{0,1}^{\mathrm{TM},2} = -ik^2 c\sqrt{\frac{\zeta}{6\pi}} p_e, \tag{40}$$

where p_e is the dipole moment. Using (36), such a dipole yields two spin coefficients

$$C_{1,0}^{E,1} = -C_{1,0}^{E,-1} = ik^3 rc\sqrt{\frac{\zeta}{12\pi}} p_e w_n^{(2)}(kr). \tag{41}$$

Asymptotically in the far-field zone, this expression becomes

$$C_{1,0}^{E,1} = -C_{1,0}^{E,-1} = -k^2 c\sqrt{\frac{\zeta}{12\pi}} p_e e^{-ikr}. \tag{42}$$

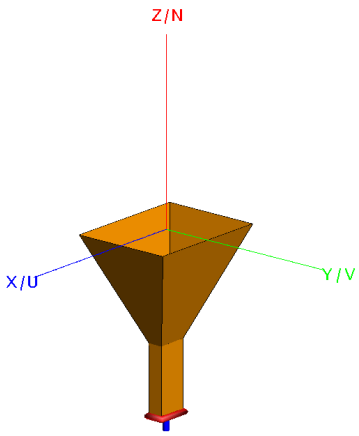

FIGURE 1. Horn antenna.

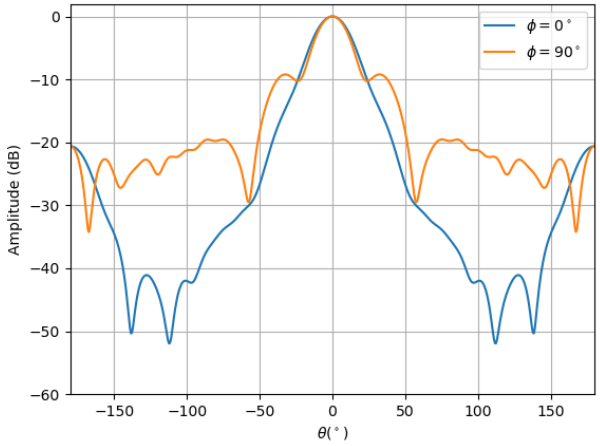

FIGURE 2. Normalized radiation pattern of the horn antenna (dB).

In a similar way, an elementary magnetic dipole of moment p_m, oriented along z and located at the origin yields two spin coefficients

$$C_{1,0}^{E,1} = C_{1,0}^{E,-1} = -ik^3 rc\sqrt{\frac{1}{12\pi\zeta}} p_m h_n^{(2)}(kr). \tag{43}$$

Asymptotically in the far-field zone, this expression becomes

$$C_{1,0}^{E,1} = C_{1,0}^{E,-1} = ik^2 c\sqrt{\frac{1}{12\pi\zeta}} p_m e^{-ikr}. \tag{44}$$

From the previous results, there exists a combination of elementary electric and magnetic dipoles which only radiates the spin harmonic $n = 1, m = 0$ and $s = -1$ or $+1$ in the far-field zone. This combination corresponds to $p_m = sip_e\zeta$. Indeed, from (42) and (44), in the far-field zone, the only non-vanishing spin coefficient in that case is

$$C_{1,0}^{E,s} = -sk^2 c\sqrt{\frac{\zeta}{3\pi}} p_e e^{-ikr}. \tag{45}$$

The far-field zone radiation is then simply given by

$$\begin{aligned} \boldsymbol{E}(r,\theta,\phi) &= -\frac{sk^2 c\zeta p_e}{\sqrt{3\pi}} Y_{s,0,1}(\theta,\phi)\frac{e^{-ikr}}{r}\hat{\boldsymbol{u}}_s(\theta,\phi) \\ &= -\frac{k^2 c\zeta p_e}{2\pi\sqrt{2}}\sin\theta\frac{e^{-ikr}}{r}\hat{\boldsymbol{u}}_s(\theta,\phi). \end{aligned} \tag{46}$$

In conclusion, balanced in-quadrature elementary electric and magnetic dipoles oriented along z produce a far-field radiation that corresponds to the harmonic $n = 1,\ m = 0$ and $s = \pm 1$.

4.2. Spin Spherical Harmonics So That n = 1 and m = ±1

As detailed in [26], a Huygens source in circular polarization can be obtained from the radiation of four co-localized elementary dipoles, whose moments are such that

$$\begin{aligned} \boldsymbol{p}_e^{(x)} &= p_e\hat{\boldsymbol{x}}, \qquad \boldsymbol{p}_m^{(x)} = sip_e\zeta\hat{\boldsymbol{x}}, \\ \boldsymbol{p}_e^{(y)} &= imp_e\hat{\boldsymbol{y}}, \quad \boldsymbol{p}_m^{(y)} = -smp_e\zeta\hat{\boldsymbol{y}}. \end{aligned} \tag{47}$$

with $s = \pm 1$ and $m = \pm 1$. In the far-field zone, this yields a circularly polarized and half-space radiation, i.e., the radiation is quasi-omnidirectional in an half-space and weak in the other half-space. The electric field is given by

$$\boldsymbol{E} = -k^2 c\zeta p_e\sqrt{2}ms\,(1 - ms\cos\theta)\,e^{im\phi}\frac{e^{-ikr}}{4\pi r}\hat{\boldsymbol{u}}_s. \tag{48}$$

This can be written as

$$\boldsymbol{E}(r,\theta,\phi) = \frac{k^2 c\zeta p_e ms\sqrt{2}}{\sqrt{3\pi}} Y_{s,m,1}(\theta,\phi)\frac{e^{-ikr}}{r}\hat{\boldsymbol{u}}_s(\theta,\phi). \tag{49}$$

This means that Huygens sources in circular polarization correspond to the spin harmonics so that $n = 1, m = \pm 1$ and $s = \pm 1$.

5. NUMERICAL ANALYSES OF ANTENNA RADIATIONS BY MEANS OF SPIN SPHERICAL HARMONICS

In this section, numerical experiments with spin spherical harmonics are performed for different types of antennas.

5.1. Rectangular Horn Antenna

The objective of the first simulation is to illustrate the use of spin spherical harmonics and to test the performances of the algorithm based on the fast spin spherical harmonic transforms. The antenna is a rectangular horn of aperture size 18 cm × 14 cm, fed by a waveguide with the TE10 mode. The far-field radiation is computed at 5 GHz with the method of moments with Altair Feko. The horn and its radiation patterns are represented in Figures 1 and 2, respectively.

The parameter N is chosen as a power of 2 to optimize fft computations, so that the criterion $N \geq kr_0 + 10$ is respected, with $r_0 = 0.27$ m the minimal radius of a sphere that includes the antenna. This criterion, which is classically used for antenna radiation, ensures that the active power is fully accounted [4]. Since here $kr_0 + 10 \approx 38.27$, we choose $N = 64$, which yields a grid with an angular step of approximately 2.83°. In

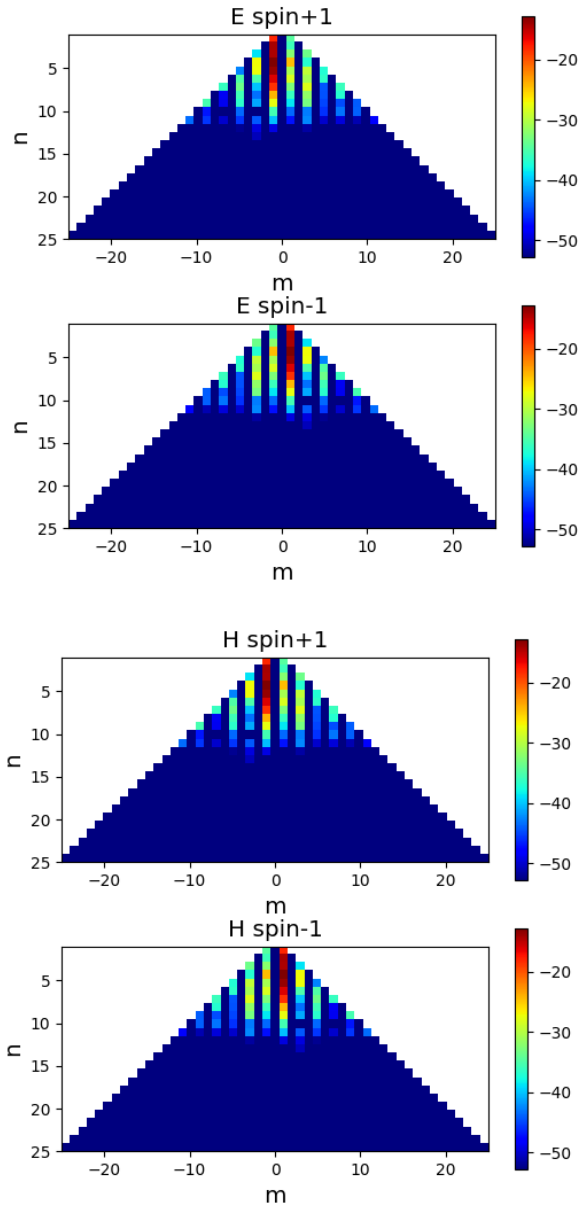

FIGURE 3. Spin spherical harmonic coefficients of a linearly polarized horn antenna (dB).

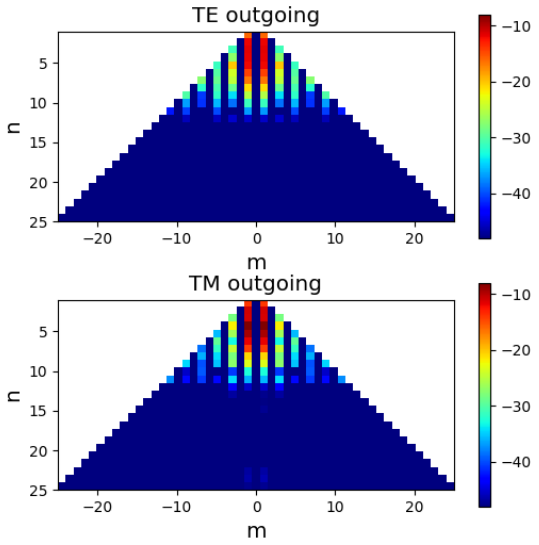

FIGURE 4. Hansen spherical harmonic coefficients of a linearly polarized horn antenna (dB).

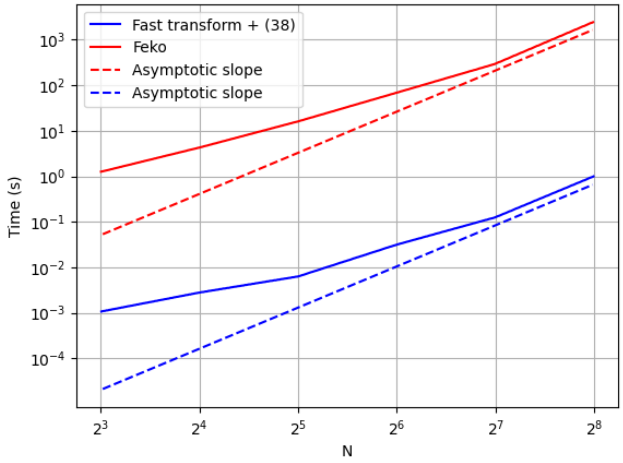

FIGURE 5. Computation times for the spherical harmonic transform.

this article, fast spin spherical harmonic transforms are computed by means of the SSHT package that is publicly available [21].

The spin harmonic coefficients are displayed in Figure 3. In this article, coefficients are displayed with a normalization so as to have a radiated power of 1 W. They become negligible from $n = 13$, which means that the band-limit has been overestimated. This notably comes from the dominant contribution in the radiation of the horn aperture, whose size is smaller than the complete antenna. Besides, coefficients of spin -1 and $+1$ are of the same order since the linearly-polarized horn radiation contains equal right-hand and left-hand circular components. Note also that only coefficients with m odd are non-zero due to the antenna symmetry. Outgoing Hansen coefficients, obtained from (38), are shown in Figure 4. The obtained ingoing coefficients are not shown since, and they are zero up to machine precision as expected for this radiation analysis.

To assess the performances of the fast transform algorithm with the conversion (38), comparisons are performed with the spherical harmonic transform of Altair Feko on an i7 16 Go laptop computer. In terms of accuracy, the root mean square difference between the two algorithms is very weak, about -85.9 dB. In terms of duration, the fast transform and Feko computation times are of 0.02 s and 80 s, respectively. Computation times for different values of N are compared in Figure 5. For both methods, the asymptotic slope corresponds to a complexity of order $\mathcal{O}(N^3)$. With the use of fast transforms, the computation time remains shorter than 1 s up to $N = 256$. Note also that for all values of N, the computation time of Feko is outperformed by a factor of at least 10^3. Thus, the fast algorithm is efficient for computing transforms with large N such as electrically large antennas.

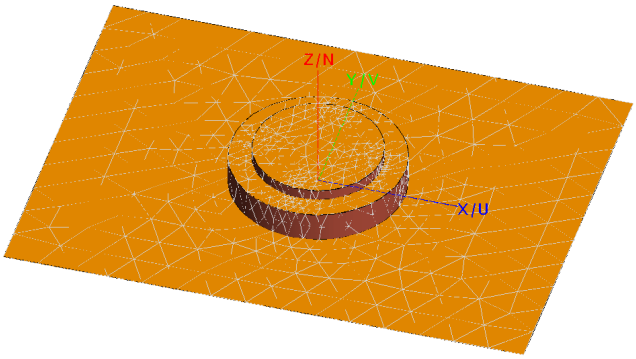

FIGURE 6. Dual-band L1-L5 stacked-patch antenna.

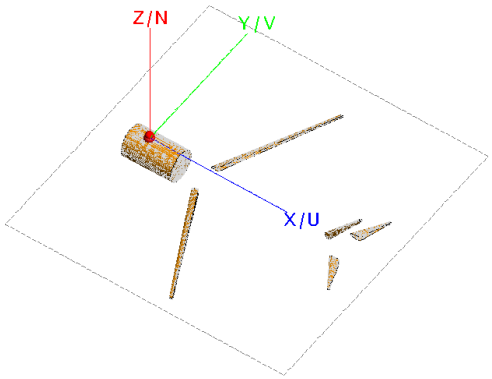

FIGURE 7. Model of the aircraft on which the antenna is simulated (fuselage, front parts of wings and stabilizers). The antenna is at the origin of the reference frame, i.e., on top of the fuselage.

5.2. GPS Antenna on an Aircraft

In the previous simulation, the fast algorithm has shown to be efficient for large values of the band-limit, up to $N = 256$. The objective of this section is to apply fast spin spherical harmonic transforms to a very large radiating system, which requires an even greater band-limit. The considered configuration is a GPS antenna installed on a single-aisle airliner. Two types of simulations are performed, with and without the airframe.

The antenna [27], shown in Figure 6, is a dual-band L1-L5 circular stacked-patch antenna, fed by 4 coaxial probes. The patches are of diameters 7.97 cm and 6.01 cm and of heights 1.4 cm and 0.5 cm, respectively. The substrate is of relative permittivity $\varepsilon_r = 4$. The size of the ground plane is 23 cm $\times$ 17 cm. For analyzing the impact on the radiation pattern of the aircraft on which the antenna is installed, a perfectly metallic airframe is added in the antenna simulation. As shown in Figure 7, only the main scattering parts of the airliner are considered in the simulation for computation purpose. The aircraft is of total length 32.7 m. The section of the fuselage on top of which the antenna is placed is modeled by a cylinder of radius 2 m and length 7 m. The front parts of the wings and horizontal stabilizers are modeled with airfoil-shaped cross sections. Their spans are 33.9 m and 12.4 m, respectively. The vertical stabilizer is of height 5.7 m.

The radiation computations are performed with Altair Feko using the method of moments for the antenna and physical optics for the aircraft. The reference frame is placed at the antenna center, at the level of the ground plane. In that frame, at the L1 center frequency $f_0 = 1.57542$ GHz, the spheres that include the antenna and aircraft are of minimal radius 0.143 m and 32 m, which corresponds to values of $kr_0 + 10$ of 15 and 1066, respectively. For capturing all the variations of the radiation in presence of the aircraft, computations are performed with $N = 2048$, which yields an angular step of approximately $0.088°$.

The computation time of the spherical harmonic transform is of 128 seconds, which remains acceptable for computing transforms from a grid implying more than 8 millions angular positions.

The radiation pattern of the antenna without the airframe at the L1 center frequency f_0 is shown in Figure 8. The co and cross polarizations of the antenna are right-hand (RHCP) and left-hand (LHCP) circular polarizations. Besides, the radiations in the $\phi = 0°$ and $\phi = 90°$ planes are very similar because of the antenna symmetry (circular patches with 4 feeding probes).

Radiations patterns when the aircraft is included in the simulation are plotted in Figure 9. There are faster variations due to the presence of the aircraft. Besides, differences appear between the $\phi = 0°$ and $\phi = 90°$ planes due to the contribution of different parts of the aircraft.

The spin spherical harmonic coefficients associated with the electric field of the antenna are displayed in Figure 10. Only coefficients of order $n \leq 15$ are displayed as higher-order coefficients are very weak. Since the main polarization of the antenna is RHCP, the strongest coefficients are associated with $+1$ spin.

The spin coefficients in presence of the aircraft are displayed in Figure 11 for orders $n \leq 80$. Even though the strongest coefficients correspond to the antenna radiation, we observe significantly more coefficients than when only the antenna is considered. It means that the scattering of elements of the aircraft introduces variations that requires higher-order spherical harmonic coefficients. Besides, when n increases, the power is distributed on a larger number of coefficients in m. Consequently, even if their amplitudes are weak, their sum can be significant and have an impact on the radiation of the antenna.

This is confirmed by Figures 12 and 13, in which the power radiated for each value of n (summing in m) is plotted without and with the aircraft. Without the aircraft, the power is concentrated on the lowest n-orders. Indeed, the power becomes negligible from $n \approx 15$, which is consistent with the band-limit criterion $kr_0 + 10$, with $r_0 = 0.143$ m the minimal radius of a sphere that includes the antenna. With the aircraft, the power is unchanged for the first orders. For higher orders, it decreases slowly up to $n \approx 150$, which corresponds to a sphere of radius 4.24 m centered on the antenna. This part of the spectrum thus includes the scattering on the aircraft fuselage. From $n \approx 150$ to $n \approx 1000$ there is a plateau of level approximately -65 dB. This part is likely due to the scattering from the aircraft components that are further from the antenna, i.e., the wings and stabilizers. The relative power associated with all the coefficients in this plateau is of order -35 dB, which means that it

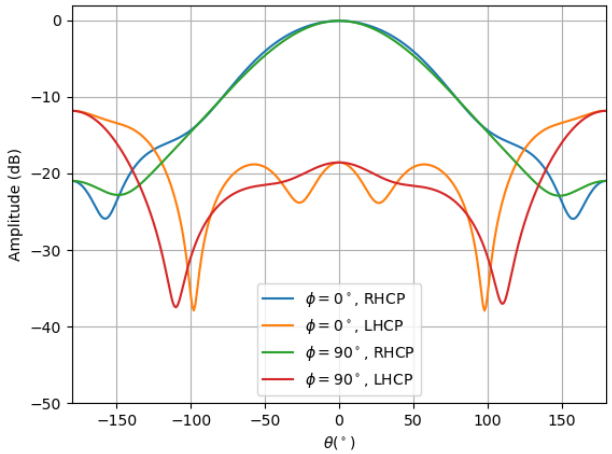

FIGURE 8. Antenna: normalized radiation patterns in co (RHCP) and cross (LHCP) polarizations for $\phi = 0°$ and $\phi = 90°$ (dB).

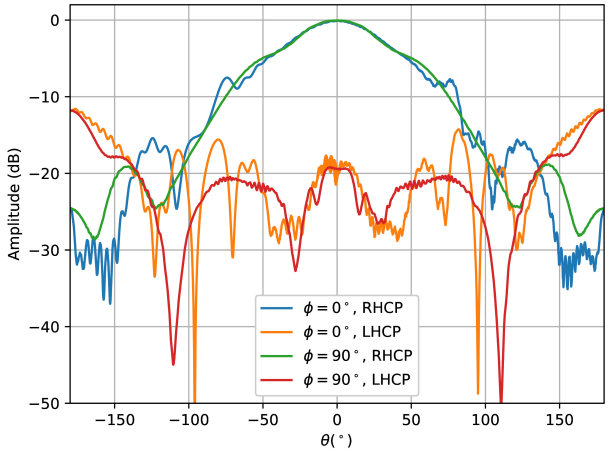

FIGURE 9. Antenna with aircraft: normalized radiation patterns in co (RHCP) and cross (LHCP) polarizations for $\phi = 0°$ and $\phi = 90°$ (dB).

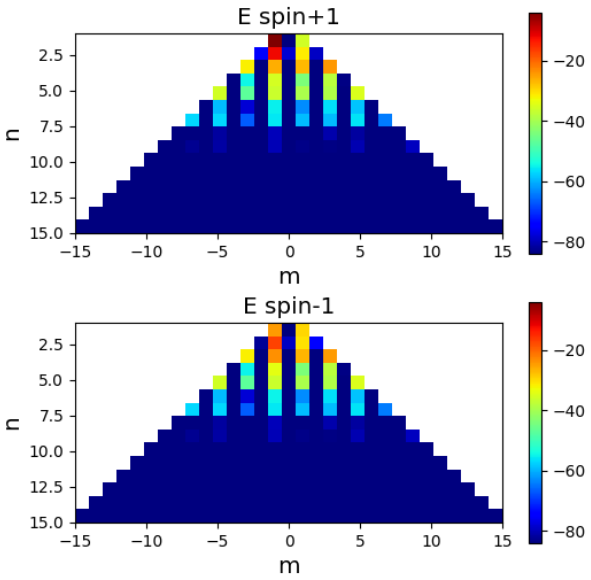

FIGURE 10. Electric spin spherical harmonic coefficients of the antenna (dB).

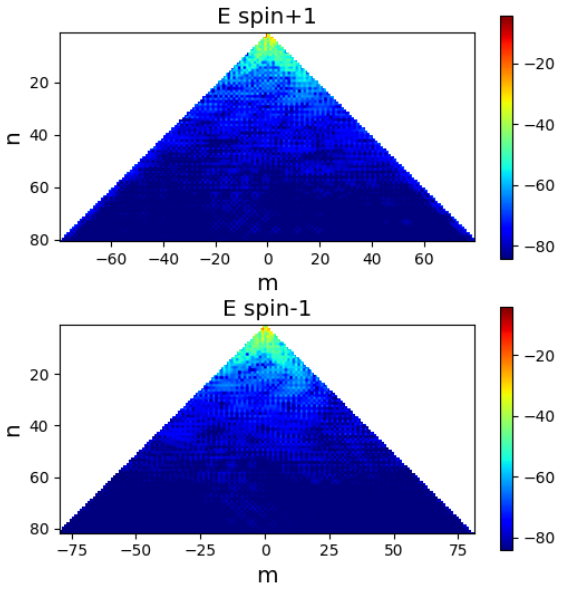

FIGURE 11. Electric spin spherical harmonic coefficients with the aircraft (dB).

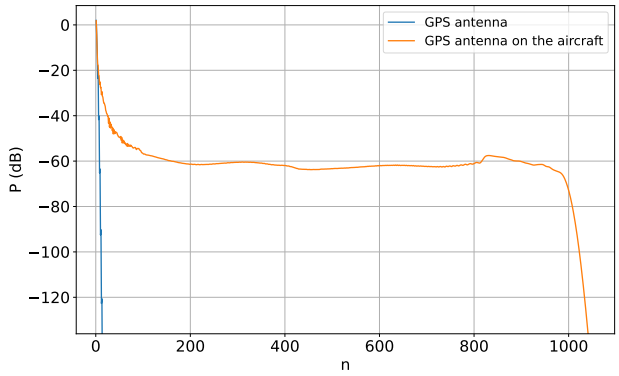

FIGURE 12. Sum in m of the spin coefficient power for each value of n.

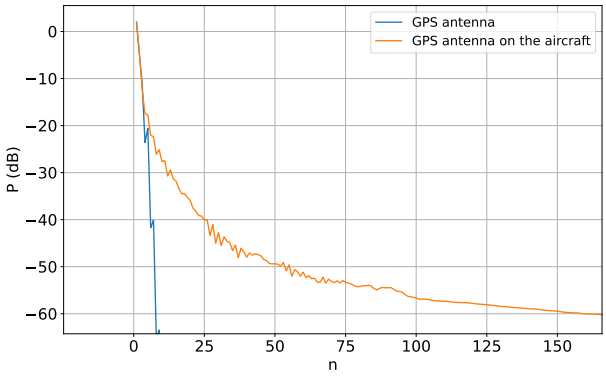

FIGURE 13. Sum in m of the spin coefficient power for $n \leq 160$.

slightly impacts the radiation. For $n \geq 1000$, the power decreases sharply, which is related to the band-limit of the complete configuration.

6. CONCLUSION

In this article, the use of spin spherical harmonics for electromagnetic radiations has been analyzed. To begin with, the theory of spin spherical harmonics have been presented. Then, vector fields tangential to a sphere have been described by means of harmonics of spin ± 1. The sampling theorem of McEwen and Wiaux and associated fast transforms have been presented. Closed-form relations between the spin spherical harmonics and Hansen spherical harmonics have been derived.

Spin spherical harmonic transforms have been applied to various radiations. The harmonics $n = 1$, $m = 0$, and $s = \pm 1$ have been related to balanced elementary electric and magnetic dipoles, while the harmonics $n = 1$, $m = \pm 1$, and $s = \pm 1$ have been related to Huygens sources in circular polarization. The efficiency of the fast spin spherical harmonic transform has been tested by means of simulations of two types of antennas: a horn antenna and a patch antenna installed on top of the fuselage of an aircraft. In all cases, harmonic coefficients for band limits N up to 2048 have been computed with computation times shorter than a few minutes.

This article has been focused on the analysis of antenna radiation by means of spin spherical harmonics. This type of harmonics could also be considered for other scattering and radiation configurations. They could also help improving the post-processing of spherical near-field antenna measurement that can be cast as a peculiar spherical deconvolution [28]. Besides, research works are currently led to quantify uncertainties in antenna radiation patterns by combining spin spherical harmonics with polynomial chaos [29].

ACKNOWLEDGEMENT

This work has been funded by the French Space Agency (CNES) and the DGA-AID, the French DOD. The view expressed in this publication can in no way be taken to reflect the opinion of the CNES.

REFERENCES

[1] Stratton, J. A., *Electromagnetic Theory*, John Wiley & Sons, 2007.

[2] Felsen, L. B. and N. Marcuvitz, *Radiation and Scattering of Waves*, John Wiley & Sons, 1994.

[3] Van Bladel, J. G., *Electromagnetic Fields*, John Wiley & Sons, 2007.

[4] Hansen, J. E., *Spherical Near-field Antenna Measurements*, IET, 1988.

[5] Ramamoorthi, R. and P. Hanrahan, "A signal-processing framework for reflection," *ACM Transactions on Graphics (TOG)*, Vol. 23, No. 4, 1004–1042, 2004.

[6] Choi, C. H., J. Ivanic, M. S. Gordon, and K. Ruedenberg, "Rapid and stable determination of rotation matrices between spherical harmonics by direct recursion," *The Journal of Chemical Physics*, Vol. 111, No. 19, 8825–8831, 1999.

[7] Ritchie, D. W. and G. J. L. Kemp, "Fast computation, rotation, and comparison of low resolution spherical harmonic molecular surfaces," *Journal of Computational Chemistry*, Vol. 20, No. 4, 383–395, 1999.

[8] Simons, F. J., F. A. Dahlen, and M. A. Wieczorek, "Spatiospectral concentration on a sphere," *SIAM Review*, Vol. 48, No. 3, 504–536, 2006.

[9] Swenson, S. and J. Wahr, "Methods for inferring regional surface-mass anomalies from Gravity Recovery and Climate Experiment (GRACE) measurements of time-variable gravity," *Journal of Geophysical Research: Solid Earth*, Vol. 107, No. B9, ETG 3–1–ETG 3–13, 2002.

[10] Whaler, K. A., "Downward continuation of Magsat lithospheric anomalies to the Earth's surface," *Geophysical Journal International*, Vol. 116, No. 2, 267–278, 1994.

[11] Turcotte, D. L., R. J. Willemann, W. F. Haxby, and J. Norberry, "Role of membrane stresses in the support of planetary topography," *Journal of Geophysical Research: Solid Earth*, Vol. 86, No. B5, 3951–3959, 1981.

[12] Wieczorek, M. A. and R. J. Phillips, "Potential anomalies on a sphere: Applications to the thickness of the lunar crust," *Journal of Geophysical Research: Planets*, Vol. 103, No. E1, 1715–1724, 1998.

[13] Bennett, C. L., A. J. Banday, K. M. Górski, G. Hinshaw, P. Jackson, P. Keegstra, A. Kogut, G. F. Smoot, D. T. Wilkinson, and E. L. Wright, "Four-year COBE* DMR cosmic microwave background observations: Maps and basic results," *The Astrophysical Journal*, Vol. 464, No. 1, L1, 1996.

[14] Jarosik, N., C. L. Bennett, J. Dunkley, B. Gold, M. R. Greason, M. Halpern, R. S. Hill, G. Hinshaw, A. Kogut, E. Komatsu, *et al.*, "Seven-year wilkinson microwave anisotropy probe (WMAP*) observations: Sky maps, systematic errors, and basic results," *The Astrophysical Journal Supplement Series*, Vol. 192, No. 2, 14, 2011.

[15] Newman, E. T. and R. Penrose, "Note on the bondi-metzner-sachs group," *Journal of Mathematical Physics*, Vol. 7, No. 5, 863–870, 1966.

[16] Matute, E. A., "On the vector solutions of Maxwell equations with the spin-weighted spherical harmonics," *ArXiv Preprint Physics/0604096*, 2006.

[17] Castillo, Torres del G. F., "Spin-weighted spherical harmonics and their applications," *Revista mexicana de física*, Vol. 53, 125–134, 2007.

[18] Shannon, C. E., "Communication in the presence of noise," *Proceedings of the IRE*, Vol. 37, No. 1, 10–21, 1949.

[19] Kowsky, W. S., "A quadrature formula over the sphere with application to high resolution spherical harmonic analysis," *Bulletin géodésique*, Vol. 60, 1–14, 1986.

[20] Driscoll, J. R. and D. M. Healy, "Computing Fourier transforms and convolutions on the 2-sphere," *Advances in Applied Mathematics*, Vol. 15, No. 2, 202–250, 1994.

[21] McEwen, J. D. and Y. Wiaux, "A novel sampling theorem on the sphere," *IEEE Transactions on Signal Processing*, Vol. 59, No. 12, 5876–5887, 2011.

[22] Mézières, N., B. Fuchs, L. L. Coq, J.-M. Lerat, R. Contreres, and G. L. Fur, "On the application of sparse spherical harmonic expansion for fast antenna far-field measurements," *IEEE Antennas and Wireless Propagation Letters*, Vol. 19, No. 5, 746–750, 2020.

[23] Price, M. A. and J. D. McEwen, "Differentiable and accelerated spherical harmonic and Wigner transforms," *Journal of Computational Physics*, Vol. 510, 113109, 2024.

[24] Mézières, N., L. L. Coq, and B. Fuchs, "Phaseless spherical near-field antenna measurements with reduced samplings," *IEEE Transactions on Antennas and Propagation*, Vol. 71, No. 9, 7447–7456, 2023.

[25] McEwen, J. D., B. Leistedt, M. Büttner, H. V. Peiris, and Y. Wiaux, "Directional spin wavelets on the sphere," *ArXiv Preprint ArXiv:1509.06749*, 2015.

[26] Morlaas, C., B. Souny, and A. Chabory, "Helical-ring antenna for hemispherical radiation in circular polarization," *IEEE Transactions on Antennas and Propagation*, Vol. 63, No. 11, 4693–4701, 2015.

[27] Macabiau, C., C. Milner, A. Chabory, N. Suard, C. Rodriguez, M. Mabilleau, J. Vuillaume, and S. Hegron, "Nominal bias analysis for ARAIM user," in *Proceedings of the 2015 International Technical Meeting of The Institute of Navigation*, 713–732, Dana Point, CA, USA, Jan. 2015.

[28] Quennelle, A., A. Chabory, R. Contreres, G. LeFur, and P. Pouliguen, "Formulation of the measurement problem and application to antenna measurement correction," in *2023 International Conference on Electromagnetics in Advanced Applications (ICEAA)*, 572–572, Venice, Italy, 2023.

[29] Djelloul, E. M., A. Chabory, C. Morlaas, and R. Douvenot, "Closed-form expression for the radiation of an arbitrarily oriented stochastic elementary dipole," in *International Conference on Electromagnetics in Advanced Applications (ICEAA)*, Palermo, Italy, 2025.